



ELSEVIER

15 October 2000

OPTICS  
COMMUNICATIONS

Optics Communications 184 (2000) 411–416

www.elsevier.com/locate/optcom

# One and two photon optogalvanic spectroscopy of argon and neon for the wavelength calibration in the near infrared

Zhen Tang<sup>\*</sup>, Richard B. Miles

*Department of Mechanical and Aerospace Engineering, Princeton University, Princeton, NJ 08544, USA*

Received 16 June 2000; accepted 23 August 2000

## Abstract

The one photon and two photon optogalvanic spectra of argon and neon have been investigated in the near infrared region between 735 and 781 nm. About 35 transitions have been recorded by illuminating a hollow cathode discharge with a pulsed Ti:sapphire laser. These transitions can serve as a convenient way to calibrate Ti:sapphire laser or optical parametric oscillator radiation in this important spectral range. © 2000 Elsevier Science B.V. All rights reserved.

## 1. Introduction

Optogalvanic spectroscopy is a well-established technique to calibrate laser wavelength in a simple but precise way. The optogalvanic effect originates from the change of impedance in a steady state gas-filled discharge when the discharge medium resonantly absorbs radiation. Radiation rearranges the excited-state populations, which in turn alters the net ionization rate of the plasma. The change of discharge impedance may be detected as a voltage change at the discharge electrodes [1–3]. The discharge impedance may be raised or lowered by the optical perturbation. The direction of the impedance change is primarily determined by the lifetime of the lower of the two states involved in the optical transition [4,5]. The accuracy of the calibration is limited to the larger of the laser line-

width or the Doppler broadening of the spectral line.

Previous optogalvanic work on argon covers the spectral regions 367–422 nm [1], 415–670 nm [2], 696–794 nm [3], and 3600–4100  $\text{cm}^{-1}$  [6]. Most of the lines detected originate from one photon transitions. Only a few one photon lines are reported in 735–781 nm region, and there are no detailed reported data for neon optogalvanic lines in this region. However, many important optical transitions occur between 735 and 781 nm and accurate wavelength calibration of Ti:sapphire laser or optical parametric oscillator radiation is a frequently encountered practical problem facing experimentalists in this spectral region.

Oxygen electronic absorption spectra of A band,  $b^1\Sigma_g^+(v' = 0) \leftarrow X^3\Sigma_g^-(v'' = 0)$ , contains a series of rotational lines from 759 to 770 nm. Quantitative detection of oxygen can be achieved by measuring the light absorption in this band with a fast response and high sensitivity [7]. Potassium atomic vapor possesses two sharp strong absorption lines at 769.90 and 766.49 nm.

<sup>\*</sup> Corresponding author. Fax: +1-609-258-1139.

E-mail address: ztang@phoenix.princeton.edu (Z. Tang).

Similarly, rubidium has transitions at 780.03 and 794.79 nm. High sensitivity rotational Raman spectra can be obtained by a combination of an atomic vapor and an infrared laser [8]. Optogalvanic calibrated atomic spectra near these transitions can be used as accurate frequency markers for these applications. Therefore, a systematical investigation has been conducted for the one photon and two photon argon and neon optogalvanic spectra in the 735–781 nm spectral region.

## 2. Experiments

The experimental setup used to detect optogalvanic spectra is shown in Fig. 1. Two Photron hollow cathode lamps were filled with argon and neon, respectively, at pressures of a few torr. Tungsten was used as the cathode material. The pulsed Ti:sapphire laser cavity is of grazing incidence design and coaxially pumped by the second harmonic of a Nd:YAG laser. The line-width of the Ti:sapphire laser is about 5 GHz. Its output is attenuated by a neutral density filter to avoid saturation. A laser pulse with tens of  $\mu\text{J}$  energy is enough to generate the optogalvanic effect. The laser beam illuminates the hollow plasma channel both with and without a focusing lens. The focusing lens is needed if the two photon optogalvanic effect is to be observed. The lamp is operated at a potential of 200–300 V which is controlled through a current limiting load resistor (about 25–50 k $\Omega$ ). The discharge current is less than 10 mA. When the laser beam is resonantly absorbed in the plasma channel, the voltage across the hollow cathode varies and this variation is coupled through a 0.0087  $\mu\text{F}$  capacitor to be recorded either by a digital oscilloscope or a BOXCAR inte-

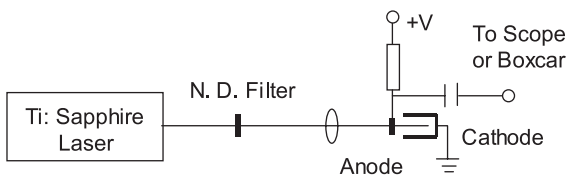


Fig. 1. Schematic diagram for the experimental setup for the laser wavelength calibration via optogalvanic effect.

grator. The digital oscilloscope captures the temporal evolution of the signal. When the Ti:sapphire laser is tuned in the resonance with a transition in the gas, the temporal signal allows the gate delay and gate width of the BOXCAR integrator to be set to optimum values to get a high sensitivity optogalvanic signal.

Figs. 2 and 3 show typical time evolution graphs for the optogalvanic signals originating from a metastable state and a non-metastable state of argon, respectively. When the laser is in resonance with an atomic line, electrons are excited to a higher level, which enhances the ionization rate, inducing a voltage drop. The characteristic recovery time of tens or hundreds of microsecond is a function of discharge parameters such as electrodes separation, fill gas pressure, discharge cur-

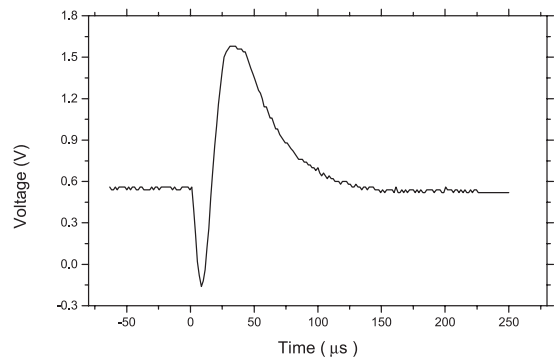


Fig. 2. Plot of typical time evolution of the optogalvanic effect signal originated from a metastable state for the lower level.

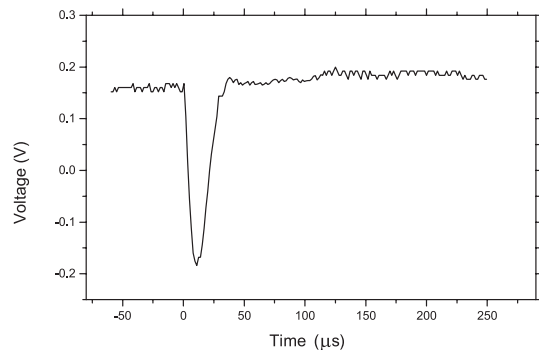


Fig. 3. Plot of typical evolution of the optogalvanic effect signal originated from a non-metastable state for the lower level.

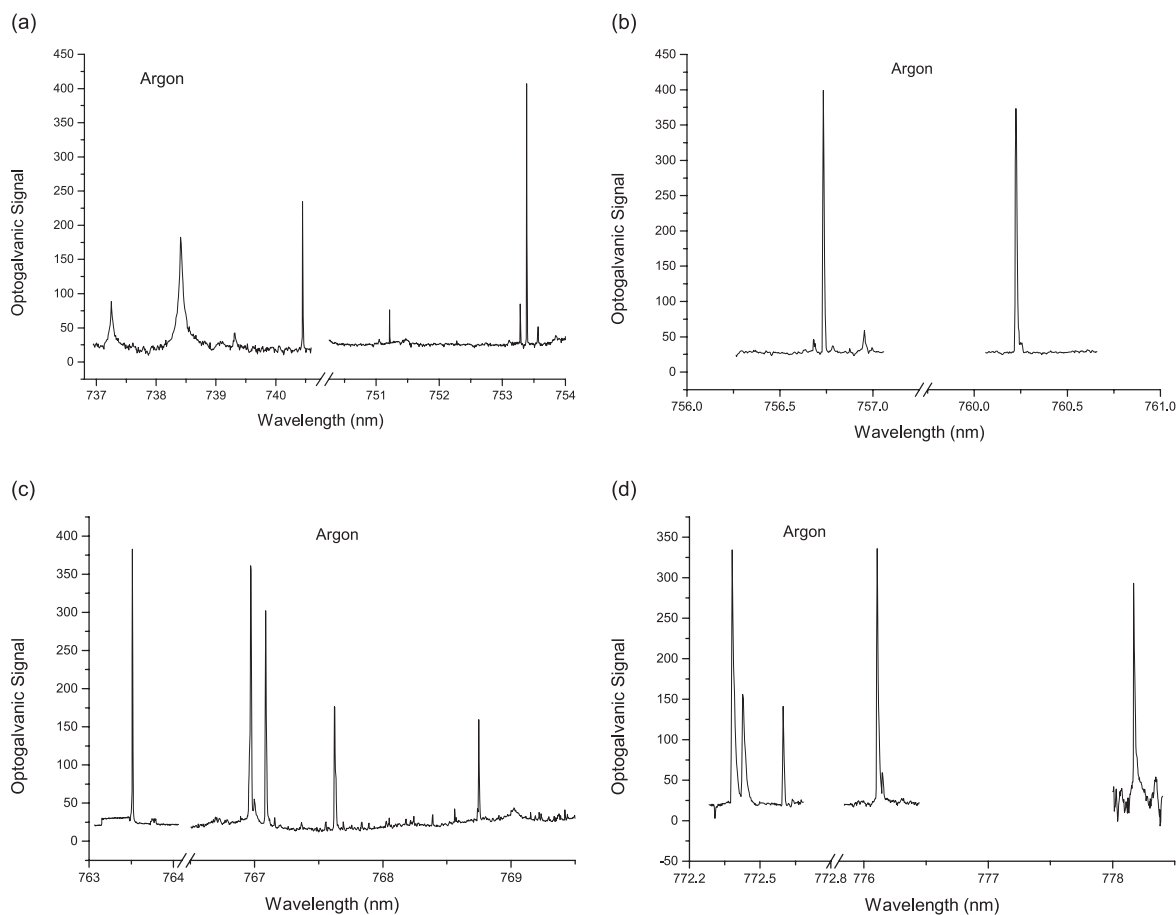


Fig. 4. Optogalvanic spectra obtained in a hollow cathode lamp filled with 1 Torr argon gas. The discharge voltage is 200 V, load resistor is 52 k $\Omega$ .

rent, and the electrical coupling circuits but not the 20 ns laser pulse duration. For a metastable lower transition level, the metastable density population is reduced by laser excitation. The lower metastable concentration forces a higher plasma sustaining voltage inducing a voltage surge. The optogalvanic signal undergoes a positive overshoot at a later time due to the relatively long relaxation time for the metastable state. For a non-metastable lower transition level, the optogalvanic voltage exhibits no overshoot.

In addition to the one photon optogalvanic effect, the two photon optogalvanic effect can be easily observed, and also used for wavelength calibration [9–11]. One photon and two photon optogalvanic signals can be distinguished from

each other by the response to light intensity. Two photon transitions can only be observed at a high laser intensity and require a focused beam. The signals from one photon and two photon optogalvanic effects are proportional to the first and second power of laser intensity respectively.

Typical optogalvanic spectra for one photon and two photon transitions obtained in argon and in neon are presented in Figs. 4 and 5.

### 3. Results and identifications

The energy structures of the noble gases (except helium) are described by the  $j_c-K$  coupling scheme [12]. The orbital angular momentum of the excited

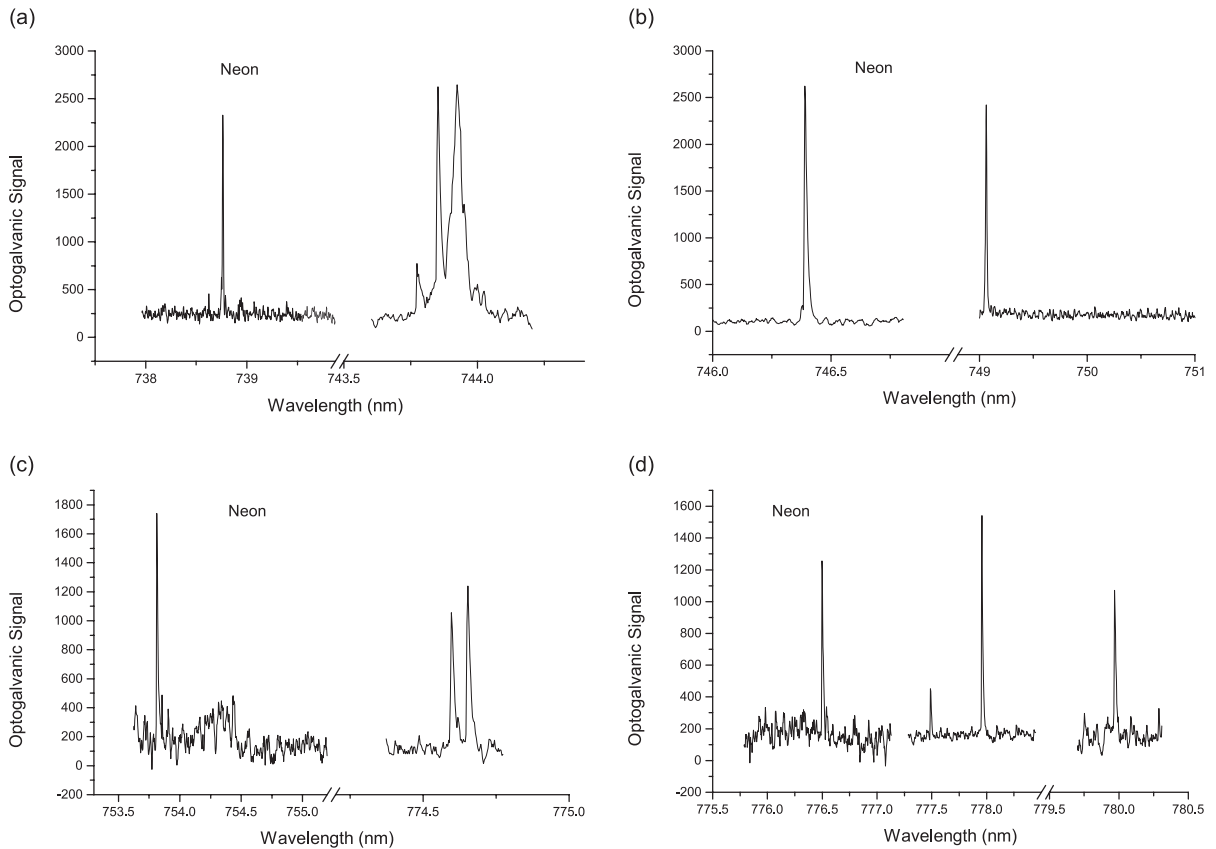


Fig. 5. Optogalvanic spectra obtained in a hollow cathode lamp filled with 1 Torr neon gas. The discharge voltage is 200 V, load resistor is 52 k $\Omega$ .

electron couples with the core angular momentum to give the angular momentum  $K$ . The  $K$  momentum finally couples with the spin of the outer electron to generate the total angular momentum  $J$  of the argon atom. The atomic energy levels are labeled by  $3p^5nI[K]_J$  or  $3p^5nI'[K]_J$  which correspond to  $j_c = 3/2$  and  $j_c = 1/2$  ionic states respectively. The singly ionized argon core,  $Ar^+$ , has the  $3p^5^2P_{3/2}$  and  $3p^5^2P_{1/2}$  odd parity states. The ionization potential for the  $3p^5^2P_{3/2}$  and  $3p^5^2P_{1/2}$  states are different: that of the  $3p^5^2P_{3/2}$  states is 127 109.88  $cm^{-1}$  and that of the  $3p^5^2P_{1/2}$  states is 128 541.41  $cm^{-1}$  [13,14]. The ground state of neutral argon is  $3p^6^1S_0$ . The atomic structure of neon is similar to that of argon. The selection rule for single-photon transition is  $\Delta J = 0, \pm 1$ . Whereas for two photon transition,  $\Delta J = 0, \pm 1, \pm 2$ .

All the observed optogalvanic transition lines in both the argon and the neon filled hollow cathode lamps are identified. The accuracy of the line assignment and wavelength measurement can be verified by simultaneously observing the emission spectrum of the discharge and the optogalvanic spectrum, and also by the signal response to the laser intensity. Many of the transition lines along with their spectral assignment are presented here for the first time, to the best of our knowledge.

Optogalvanic spectra for the calibration of laser wavelength can provide very accurate wavelength markers, good to at least six significant digits. The optogalvanic effect relies on standard electrical measurement techniques avoiding optical problems such as laser elastic background and collection efficiency. Consequently, it can detect weak

Table 1  
Argon optogalvanic lines along with their transition assignment in the near infrared spectral region

Wavelength (nm)	$E_{\text{lower}} \text{ (cm}^{-1}\text{)}$	$E_{\text{upper}} \text{ (cm}^{-1}\text{)}$	Transition identification	Transition type
737.212	105 462	119 024	$3p^5 4p \left[ \frac{3}{2} \right]_3 - 3p^5 4d \left[ \frac{7}{2} \right]_4$	One photon
738.398	93 751	107 290	$3p^5 4s \left[ \frac{3}{2} \right]_1 - 3p^5 4p' \left[ \frac{3}{2} \right]_2$	One photon
739.297	106 238	119 760	$3p^5 4p \left[ \frac{3}{2} \right]_2 - 3p^5 6s \left[ \frac{3}{2} \right]_1$	One photon
740.454	93 751	120 753	$3p^5 4s \left[ \frac{3}{2} \right]_1 - 3p^5 4d' \left[ \frac{7}{2} \right]_3$	Two photon
751.208	93 144	119 760	$3p^5 4s \left[ \frac{3}{2} \right]_2 - 3p^5 6s \left[ \frac{3}{2} \right]_1$	Two photon
753.288	94 553	121 097	$3p^5 4s' \left[ \frac{1}{2} \right]_0 - 3p^5 6s' \left[ \frac{3}{2} \right]_0$	Two photon
753.391	93 144	119 683	$3p^5 4s \left[ \frac{3}{2} \right]_2 - 3p^5 6s \left[ \frac{3}{2} \right]_2$	Two photon
753.570	95 399	121 932	$3p^5 4s' \left[ \frac{1}{2} \right]_1 - 3p^5 5d' \left[ \frac{11}{2} \right]_1$	Two photon
756.729	93 144	119 566	$3p^5 4s \left[ \frac{3}{2} \right]_2 - 3p^5 4d \left[ \frac{7}{2} \right]_3$	Two photon
760.217	93 144	119 445	$3p^5 4s \left[ \frac{3}{2} \right]_2 - 3p^5 4d \left[ \frac{7}{2} \right]_2$	Two photon
763.511	93 144	106 238	$3p^5 4s \left[ \frac{3}{2} \right]_2 - 3p^5 4p \left[ \frac{3}{2} \right]_2$	Two photon
766.983	93 144	119 213	$3p^5 4s \left[ \frac{3}{2} \right]_2 - 3p^5 4d \left[ \frac{7}{2} \right]_3$	Two photon
767.094	94 554	120 619	$3p^5 4s' \left[ \frac{1}{2} \right]_0 - 3p^5 4d' \left[ \frac{7}{2} \right]_2$	Two photon
767.628	94 554	120 601	$3p^5 4s' \left[ \frac{1}{2} \right]_0 - 3p^5 4d' \left[ \frac{7}{2} \right]_2$	Two photon
768.740	93 751	119 760	$3p^5 4s \left[ \frac{3}{2} \right]_1 - 3p^5 6s \left[ \frac{3}{2} \right]_1$	Two photon
772.376	93 144	106 087	$3p^5 4s \left[ \frac{3}{2} \right]_2 - 3p^5 4p \left[ \frac{3}{2} \right]_1$	One photon
772.421	94 554	107 496	$3p^5 4s' \left[ \frac{1}{2} \right]_0 - 3p^5 4p' \left[ \frac{3}{2} \right]_1$	One photon
772.593	93 144	119 024	$3p^5 4s \left[ \frac{3}{2} \right]_2 - 3p^5 4d \left[ \frac{7}{2} \right]_4$	Two photon
776.104	93 144	118 907	$3p^5 4s \left[ \frac{3}{2} \right]_2 - 3p^5 4d \left[ \frac{7}{2} \right]_2$	Two photon
778.177	93 751	119 445	$3p^5 4s \left[ \frac{3}{2} \right]_1 - 3p^5 4d \left[ \frac{7}{2} \right]_2$	Two photon

The second and third column are the energy of lower and upper level respectively.

Table 2  
Neon optogalvanic lines along with their transition assignment in the near infrared spectral region

Wavelength (nm)	$E_{\text{lower}} \text{ (cm}^{-1}\text{)}$	$E_{\text{upper}} \text{ (cm}^{-1}\text{)}$	Transition identification	Transition type
738.757	134 459	161 524	$2p^5 3s \left[ \frac{3}{2} \right]_1 - 2p^5 3d \left[ \frac{1}{2} \right]_1$	Two photon
743.762	134 819	161 701	$2p^5 3s' \left[ \frac{1}{2} \right]_0 - 2p^5 3d \left[ \frac{5}{2} \right]_3$	Two photon
743.811	134 819	161 700	$2p^5 3s' \left[ \frac{1}{2} \right]_0 - 2p^5 3d \left[ \frac{5}{2} \right]_2$	Two photon
743.890	134 819	148 258	$2p^5 3s' \left[ \frac{1}{2} \right]_0 - 2p^5 3p \left[ \frac{1}{2} \right]_1$	One photon
746.378	134 819	161 607	$2p^5 3s' \left[ \frac{1}{2} \right]_0 - 2p^5 3d \left[ \frac{7}{2} \right]_3$	Two photon
749.109	134 819	161 510	$2p^5 3s' \left[ \frac{1}{2} \right]_0 - 2p^5 3d \left[ \frac{1}{2} \right]_0$	Two photon
753.577	148 258	161 510	$2p^5 3p \left[ \frac{1}{2} \right]_1 - 2p^5 3d \left[ \frac{1}{2} \right]_0$	One photon
774.603	135 889	161 701	$2p^5 3s' \left[ \frac{1}{2} \right]_1 - 2p^5 3d \left[ \frac{5}{2} \right]_3$	Two photon
774.657	135 889	161 700	$2p^5 3s' \left[ \frac{1}{2} \right]_1 - 2p^5 3d \left[ \frac{5}{2} \right]_2$	Two photon
776.554	135 889	161 637	$2p^5 3s' \left[ \frac{1}{2} \right]_1 - 2p^5 3d \left[ \frac{3}{2} \right]_1$	Two photon
777.441	135 889	161 607	$2p^5 3s' \left[ \frac{1}{2} \right]_1 - 2p^5 3d \left[ \frac{3}{2} \right]_2$	Two photon
777.953	135 889	161 590	$2p^5 3s' \left[ \frac{1}{2} \right]_1 - 2p^5 3d \left[ \frac{7}{2} \right]_4$	Two photon
779.961	135 889	161 524	$2p^5 3s' \left[ \frac{1}{2} \right]_1 - 2p^5 3d \left[ \frac{1}{2} \right]_1$	Two photon

The second and third column are the energy of lower and upper level respectively.

transitions with high signal to noise ratio. Two photon optogalvanic spectra provide new wavelength markers in addition to the lines which can be observed in emission or fluorescence spectra. Tables 1 and 2 summarize the optogalvanic lines observed in argon and neon along with their transition identifications. All the observed lines are transition associated with neutral argon or neon atoms.

#### 4. Conclusions

Thirty five lines of one photon and two photon optogalvanic spectra of argon and neon were observed and assigned in the 735–781 nm spectral region. These lines are accurate to six significant digits, and are suitable as inexpensive and convenient calibration wavelength markers of Ti:sapphire or optical parametric oscillator radiation.

**References**

- [1] M. Hippler, J. Pfab, *Opt. Commun.* 97 (1993) 347.
- [2] B.R. Reddy, P. Venkateswarlu, M.C. George, *Opt. Commun.* 75 (1990) 267.
- [3] J.R. Nestor, *Appl. Opt.* 21 (1982) 4154.
- [4] G. Erez, S. Lavi, E. Miron, *IEEE J. Quant. Electron.* QE-15 (1979) 1328.
- [5] E. Miron, I. Smilanski, J. Liran, S. Lavi, G. Erez, *IEEE J. Quant. Electron.* QE-15 (1979) 194.
- [6] M.H. Begemann, R.J. Saykally, *Opt. Commun.* 40 (1982) 277.
- [7] M. Kroll, J.A. McClintock, O. Ollinger, *Appl. Phys. Lett.* 51 (1987) 1465.
- [8] A. Nohe, G. Lermann, H. Schwoerer, W. Kiefer, J. Sawatzki, G. Surawicz, *J. Mol. Struct.* 410–411 (1997) 65.
- [9] N.K. Piracha, B. Suleman, S.H. Khan, M.A. Baig, *J. Phys. B* 28 (1995) 2525.
- [10] N.K. Piracha, M.A. Baig, S.H. Khan, B. Suleman, *J. Phys. B* 30 (1997) 1151.
- [11] M. Ahmed, M.A. Zia, M.A. Baig, B. Suleman, *J. Phys. B* 30 (1997) 2155.
- [12] R.D. Cowan, *The Theory of Atomic Structure and Spectra*, University of California Press, Berkeley, CA, 1981.
- [13] M. Pellarin, J.L. Vialle, M. Carre, J. Lerme, M. Aymar, *J. Phys. B* 21 (1988) 3833.
- [14] J. Landais, M. Huet, H. Kucal, T. Dohnalik, *J. Phys. B* 28 (1995) 2395.